

## Anomalous Diffusion and Electrical Response of Ionic Solutions

E. K. Lenzi<sup>1</sup>, P. R. G. Fernandes<sup>1</sup>, T. Petrucci<sup>1</sup>, H. Mukai<sup>1</sup>, H. V. Ribeiro<sup>1</sup>, M. K. Lenzi<sup>1</sup>, G. Gonçalves<sup>3</sup>

<sup>1</sup> Departamento de Física, Universidade Estadual de Maringá, Avenida Colombo 5790, 87020 - 900 Maringá - PR, Brazil.

<sup>2</sup> Departamento de Engenharia Química, Universidade Federal do Paraná, Setor de Tecnologia - Jardim das Américas, Caixa Postal 19011, 81531 - 990, Curitiba - PR, Brazil.

<sup>3</sup> Departamento de Engenharia Química, Universidade Estadual de Maringá, Avenida Colombo 5790, 87020-900, Maringá - PR, Brazil.

\*E-mail: [eklenzi@dfi.uem.br](mailto:eklenzi@dfi.uem.br)

Received: 2 December 2012 / Accepted: 22 December 2012 / Published: 1 February 2013

---

We analyze the electrical response obtained in the framework of a model in which the diffusion of mobile ions in the bulk is governed by a fractional diffusion equation of distributed order subjected to integro-differential boundary conditions. The analysis is carried out by supposing that the positive and negative ions have different mobility and that the electric potential profile across the sample satisfies the Poisson's equation. In addition, we also compare the analytical results with experimental data obtained from ionic solutions of a salt dissolved in water, revealing a good agreement and evidencing that the dynamics of the ions can be related to different diffusive processes and, consequently, to anomalous diffusion.

---

**Keywords:** anomalous diffusion; electrical response; fractional diffusion equations; ionic solution

PACS Numbers: 05.40.Jc, 66.10.-x, 05.40.Fb, 68.08.-p, 84.37.+q

### 1. INTRODUCTION

Since the work of the botanic Robert Brown [1] on the thermal motion of small particles and the explanation proposed by Albert Einstein [2], the diffusive phenomenon has been widely investigated in several fields of science, in particular the ones where the anomalous diffusion is present. For instance, in atom deposition into a porous substrate [3], ultracold atoms [4], diffusion of high molecular weight polyisopropylacrylamide in nanopores [5], highly confined hard disk fluid mixtures [6], viscosity landscapes [7], fluctuating particle fluxes [8], granular materials [9], diffusion on fractals [10,11], ferrofluid [12], p-doped poly(3,4- ethylenedioxythiophene) modified electrodes [13], colloids [14], micromechanical responses of breast cancer cells and adjacent fibroblasts [15], and

many others. Depending on the nature of the stochastic process connected to the phenomenon in analysis, either Markovian [16] or non Markovian [17,18] features can be observed. In the last scenario, the spreading of the system is characterized by a nonlinear time dependence for the mean square displacement, e.g.,  $\langle (z - \langle z \rangle)^2 \rangle \sim t^\gamma$ , as a result of, for example, memory effects [18,19], long-range correlations, long-range interactions [20-22], or surface effects [23,24]. In this context, the electrical response of several systems (see Refs. [25-30]) may find a suitable description since the usual formalism, essentially connected to a Markovian process, does not conveniently describe the experimental results. Therefore, not only the boundary conditions connected to the surface effects, which play a significant role in the electric response, but also the bulk equations should be revisited. In this sense, Bisquert, Compte, and coworkers [31-34] were the first to apply the fractional diffusion equation which, afterwards, has been worked out in the presence of the Poisson equation [35-37]. These results, based on the fractional approach [38-40], represent a new possibility when investigating different scenarios or revisiting physical situations, which are not suitably described in terms of the standard formalism. One of these scenarios is the electrical response obtained from ionic solutions, salt dissolved in water, which shows unusual diffusive regimes similar to the ones observed in Refs. [26,27] for water.

The plan of this work is first to analyze a model based on fractional diffusion equations of distributed order taking into account different mobilities (diffusion coefficients) and surface effects represented by the boundary conditions. This analysis is performed in Sec. 2 and extends the discussion present in Refs. [28,35,37] to a general case. Next, in Sec. 3, the phenomenological model is compared with experimental data obtained from the ionic solutions of  $KClO_3$  dissolved in Milli-Q deionized water, i.e., ultrapure water of Type 1 according to the standards, for the complex dielectric constant (permittivity) ( $\varepsilon = \varepsilon' + i\varepsilon''$ ). The agreement between the phenomenological model and the experimental data suggests that the dynamic of the ions, i.e., the diffusion process, is anomalous, similarly to the cases analyzed in Refs. [27,28]. The two last sections, Sec. 4 and Sec. 5, are devoted to discussions and conclusions.

## 2. PHENOMENOLOGICAL FRAMEWORK

Let us start our discussion presenting the phenomenological model that will be used to investigate our experimental data presented in the next section. Following the developments performed in Refs. [27,28,37], we consider a fractional diffusion equation of distributed order [41] for the bulk density of ions  $n_\alpha$  ( $\alpha = +$  for positive and  $\alpha = -$  for negative ones),

$$\left( \mathcal{A} \frac{\partial}{\partial t} + \mathcal{B} \frac{\partial^\gamma}{\partial t^\gamma} \right) n_\alpha(z, t) = - \frac{\partial}{\partial z} J_\alpha(z, t) \quad (1)$$

where  $\mathcal{A} + \mathcal{B} = 1$ ,  $\gamma$  is real number in the range  $0 < \gamma \leq 2$ , and the current density given by

$$J_\alpha(z,t) = -\mathcal{D}_\alpha \frac{\partial}{\partial z} n_\alpha(z,t) \mp \frac{q\mathcal{D}_\alpha}{k_B T} n_\alpha(z,t) \frac{\partial}{\partial z} V(z,t) \tag{2}$$

Note that  $1 < \gamma$  in Eq. (1) introduces a finite phase velocity which implies in a finite collision time, which is not present in the usual diffusion equation. Indeed, the usual diffusion equation is an approximation only valid in time scales that are large when compared with the time scale in which the diffusion-causing collisions takes place. In fact, the most striking non-physical properties of the standard diffusion equation is the infinite velocity of information propagation. In addition, Eq. (1) may also be connected to the situations discussed in Refs. [42-44] which are essentially non-Markovian. In Eq.(2),  $\mathcal{D}_\alpha$  is the diffusion coefficient for the mobile ions (the same for positive and negative ones) of charge  $q$ ,  $V$  is the actual electric potential across a sample of thickness  $d$ , with the electrodes placed at the positions  $z = \pm d/2$  of a Cartesian reference frame where  $z$  is the axis normal to them,  $k_B$  is the Boltzmann constant, and  $T$  is absolute temperature. The fractional operator considered here is the Caputo's one [45], i.e.,

$$\frac{\partial^\gamma}{\partial t^\gamma} n_\alpha(z,t) = \frac{1}{\Gamma(k-\gamma)} \int_{t_0}^t dt' \frac{n_\alpha^{(k)}(z,t')}{(t-t')^{\gamma-n+1}} \tag{3}$$

with  $k-1 < \gamma < k$  and  $n_\alpha^{(k)}(z,t) \equiv \partial_t^k n_\alpha(z,t)$ . In particular, we consider  $t_0 \rightarrow -\infty$  to analyze the response of the system under a periodic potential applied, defined later on, as indicated by Ref. [45]. In order to cover the influence of the surface on the ions in a more general situation, we consider that Eq. (1) is subjected to the boundary condition

$$J_\alpha(z,t)|_{z=\pm d/2} = \pm \int_0^1 d\vartheta \int_{-\infty}^t dt' \bar{\kappa}_\alpha(t-t',\vartheta) \frac{\partial^\vartheta}{\partial t'^\vartheta} n_\alpha(z,t') \Big|_{z=\pm d/2} . \tag{4}$$

Equation (4) recovers several situations such as the blocking electrodes for  $\bar{\kappa}_\alpha(t,\vartheta) = 0$ , adsorption-desorption process at the surfaces corresponding to the Langmuir approximation when  $\bar{\kappa}_\alpha(t,\vartheta) \propto e^{-t'/\tau} \delta(\vartheta-1)$  [46], and a Chang-Jaffe like boundary condition for  $\bar{\kappa}_\alpha(t,\vartheta) \propto \delta(t)\delta(\vartheta)$ . In this manner, Eq. (4) allows a unified framework for dealing with several boundary conditions and also with nonusual relaxations [24] which emerge when  $\bar{\kappa}_\alpha(t,\vartheta) \propto \kappa(t)\delta(\vartheta)$  for  $\kappa(t)$  arbitrary. For  $\bar{\kappa}_\alpha(t,\vartheta) \propto \delta(t)\tilde{\tau}(\vartheta)$  with  $\tilde{\tau}(\vartheta)$  arbitrary, we can related the processes at the surface with fractional kinetic equations [47,48]. These anomalous processes may also be related to the effects produced by the roughness of the surface in the limit of low frequency, leading us to obtain a power law behavior for the electric response, similar to the ones reported in Refs. [49] and [50]. Hence, the boundary condition considered here may interpolate several contexts which play an important role describing the electrical response of the system and, consequently, may be useful to investigate the system where the nonusual behavior is manifested. The potential is determined by the Poisson's equation

$$\frac{\partial^2}{\partial z^2} V(z,t) = -\frac{q}{\mathfrak{m}} [n_+(z,t) - n_-(z,t)] \tag{5}$$

which depends on the difference between the densities of the charged particles. From this equation, we may obtain the impedance ( $Z$ ) and, consequently, the quantities  $\epsilon'$  and  $\epsilon''$  connected to the complex dielectric constant. In particular, we have that

$$\epsilon' = -\frac{d}{\omega S} \frac{\mathcal{X}}{\mathcal{X}^2 + \mathcal{R}^2} \tag{6}$$

$$\epsilon'' = \frac{d}{\omega S} \frac{\mathcal{R}}{\mathcal{X}^2 + \mathcal{R}^2} \tag{7}$$

where  $\mathcal{X} = \text{Im} Z$ ,  $\mathcal{R} = \text{Re} Z$ ,  $S$  is the area of the electrode, and  $d$  is the thickness of the sample. The real part,  $\epsilon'$ , is connected with the usual dielectric properties of the medium, whereas the imaginary part,  $\epsilon''$ , is related to the relative dielectric loss factor. In particular, the imaginary part,  $\epsilon''$ , is related to the conductivity of the system by the relation  $\sigma = \omega \epsilon''$ .

Let us obtain an expression for the electrical impedance for investigating the experimental data in connection to Eqs. (6) and (7). In this sense, we consider Eq.(1) subjected to Eqs. (4) and (5) in the linear approximation by considering that  $n_\alpha(z,t) = \mathcal{N} + \delta n_\alpha(z,t)$ , with  $\mathcal{N} \gg \delta n_\alpha(z,t)$  where  $\mathcal{N}$  represents the number of ions. In addition, we also consider  $\delta n_\alpha(z,t) = \eta_\alpha(z) e^{i\omega t}$  to analyze the impedance when the electrolytic cell is subjected to the time dependent potential  $V(z,t) = \phi(z) e^{i\omega t}$ , with  $V(\pm d/2, t) = \pm V_0 e^{i\omega t} / 2$ . After substituting these quantities in Eqs. (1), (4), and (5), we obtain a set of coupled equations which have the following solution for  $\eta_+(z)$  and  $\eta_-(z)$

$$\eta_+(z) = C_{+,1} e^{\delta_1 z} + C_{+,2} e^{-\delta_1 z} + C_{+,3} e^{\delta_2 z} + C_{+,4} e^{-\delta_2 z} \tag{8}$$

$$\eta_-(z) = C_{-,1} e^{\delta_1 z} + C_{-,2} e^{-\delta_1 z} + C_{-,3} e^{\delta_2 z} + C_{-,4} e^{-\delta_2 z} \tag{9}$$

with

$$\frac{C_{-,1}}{C_{+,1}} = \frac{C_{-,2}}{C_{+,2}} = -2\lambda^2 (\delta_1^2 - \xi_+^2) = k_1 \tag{10}$$

$$\frac{C_{-,3}}{C_{+,3}} = \frac{C_{-,4}}{C_{+,4}} = -2\lambda^2 (\delta_2^2 - \xi_+^2) = k_2 \tag{11}$$

where

$$\delta_{1,2} = \pm \sqrt{\frac{1}{2} (\xi_+^2 + \xi_-^2) \pm \frac{1}{2} \sqrt{(\xi_+^2 - \xi_-^2)^2 + 4\beta^2}} \tag{12}$$

with  $\xi_\alpha = 1/(2\lambda^2) + i\omega/D_\alpha$ ,  $\beta = 1/(2\lambda^2)$ , and  $\lambda = \sqrt{\mathfrak{M}_B T / (2\mathcal{N}q^2)}$ . By using the previous equation it is possible to show that the potential for this system is given by

$$\phi(z) = -\frac{q}{\mathfrak{M}} \left\{ \frac{1-k_1}{\delta_1^2} (C_{+,1} e^{\delta_1 z} + C_{+,2} e^{-\delta_1 z}) + \frac{1-k_2}{\delta_2^2} (C_{+,3} e^{\delta_2 z} + C_{+,4} e^{-\delta_2 z}) \right\} + \mathcal{A}z + \mathcal{B}. \tag{13}$$

Equations (8), (9), and (13) may also be simplified by applying the condition  $\phi(z) = -\phi(-z)$ ,

$$\eta_+(z) = 2C_{+,1} \sinh(\delta_1 z) + 2C_{-,3} + \sinh(\delta_2 z) \quad , \tag{14}$$

$$\eta_-(z) = 2k_1 C_{+,1} \sinh(\delta_1 z) + 2k_2 C_{-,3} + \sinh(\delta_2 z) \quad , \tag{15}$$

$$\phi(z) = -\frac{q}{\mathfrak{M}} 2 \left\{ \frac{1-k_1}{\delta_1^2} C_{+,1} \sinh(\delta_1 z) + \frac{1-k_2}{\delta_2^2} C_{+,3} \sinh(\delta_2 z) \right\} + \mathcal{A}z. \tag{16}$$

In order to obtain a relation between  $C_{+,1}$  and  $C_{+,3}$ , Eq. (4) can be used accomplishing the linear approximation, yielding

$$C_{+,3} = -\Lambda(i\omega)C_{+,1} \tag{17}$$

with

$$\Lambda(i\omega) = \frac{(1+k_1)\delta_1 \cosh(\delta_1 d/2) + (\Phi_+(i\omega) + k_1\Phi_-(i\omega))\sinh(\delta_1 d/2)}{(1+k_2)\delta_2 \cosh(\delta_2 d/2) + (\Phi_+(i\omega) + k_2\Phi_-(i\omega))\sinh(\delta_2 d/2)}, \tag{18}$$

where  $\Phi_\alpha(i\omega) = \int_0^1 d\mathcal{G} \int_0^\infty dv (i\omega)^{\mathcal{G}} e^{-i\omega v} \bar{\kappa}_\alpha(v, \mathcal{G})$ . By using Eq.(17) and the boundary conditions, it is possible to show that

$$\mathcal{A} = -\frac{4\lambda^2 q}{\mathfrak{M}} \mathcal{F}(i\omega)C_{+,1} \quad , \tag{19}$$

$$C_{+,3} = -V_0 \frac{\mathfrak{M}}{4\lambda^2 q d} \frac{1}{\Lambda(i\omega) + \mathcal{F}(i\omega)} \quad , \tag{20}$$

where

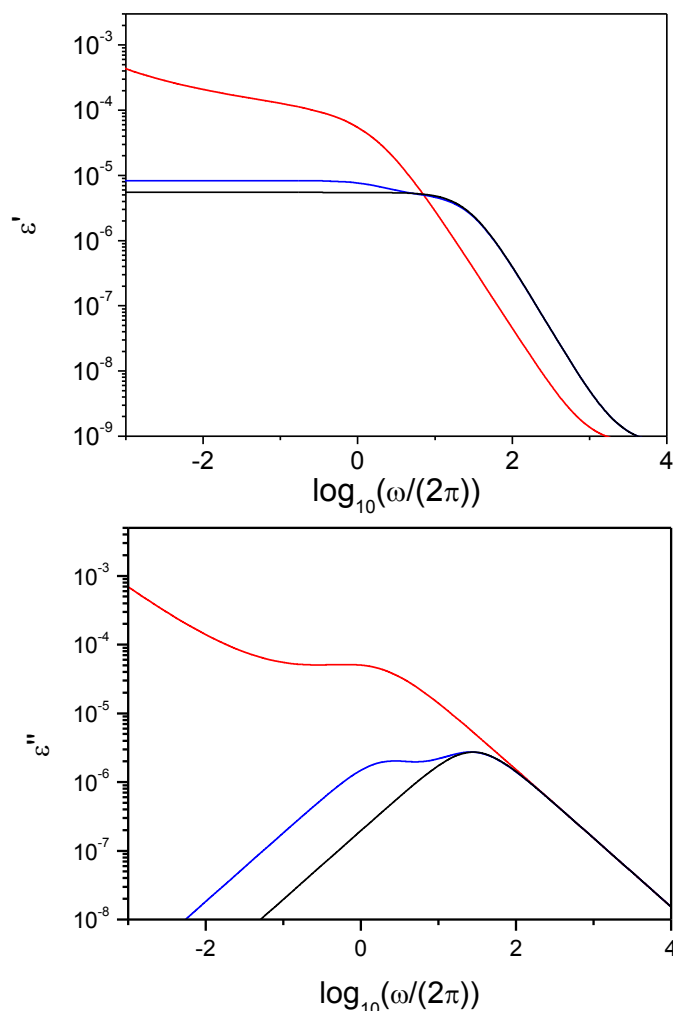


**Figure 1.** Behavior of the real and imaginary parts of the complex dielectric constant. The red line corresponds to the model presented here, the black line is the case of perfect blocking electrodes and the blue line is the case characterized by adsorption. The values adopted for the parameters are  $\kappa_1 = 2.9 \times 10^{-4}$  m/s,  $\kappa_2 = 3.48 \times 10^{-7}$  m/s,  $\kappa_3 = 4.62 \times 10^{-7}$  m/s,  $\lambda = 1.03 \times 10^{-7}$  m,  $\tau = 2 \times 10^{-3}$  s,  $\tau_3 = 0.076$  s,  $\eta_1 = 0.155$ ,  $\eta_2 = 0.88$ ,  $\mathcal{D}_+ = \mathcal{D}_- = 6 \times 10^{-9} \text{ m}^2 / \text{s}$ , and  $\mathbb{M}_{\pm} = 85 \mathbb{M}_{\pm}$  (where  $\mathbb{M}_{\pm} = 8.815 \times 10^{-12} \text{ C}^2 / (\text{N m}^2)$ ).

$$\begin{aligned}
 F(i\omega) = & \left( \delta_1 - \frac{1-k_1}{2\delta_1\lambda^2} \right) \cosh\left( \delta_1 \frac{d}{2} \right) - \left( \delta_2 - \frac{1-k_2}{2\delta_2\lambda^2} \right) \Lambda(i\omega) \cosh\left( \delta_2 \frac{d}{2} \right) \\
 & + \Phi_+(i\omega) \left( \sinh\left( \delta_1 \frac{d}{2} \right) - \Lambda(i\omega) \cosh\left( \delta_2 \frac{d}{2} \right) \right)
 \end{aligned} \tag{21}$$

and

$$\Lambda(i\omega) = \frac{1-k_1}{2\delta_1^2\lambda^2 d} \sinh\left( \delta_1 \frac{d}{2} \right) - \frac{1-k_2}{2\delta_2^2\lambda^2 d} \Lambda(i\omega) \sinh\left( \delta_2 \frac{d}{2} \right) \quad . \tag{22}$$

From the previous results, it is possible to obtain the electric field  $E(z,t)$  and, consequently, from the Coulomb theorem  $E(d/2,t) = -\Sigma(t)/\epsilon_0$ , where  $\Sigma$  is the surface density of charge on the electrode at  $z = d/2$ . These quantities are relevant to obtain the admittance  $\mathcal{Y}$  and, consequently, the impedance  $Z = 1/\mathcal{Y}$  of the system. The current at the electrode is determined by the equation  $I = Sq(j_+ - j_-) + Sd\Sigma/dt$  from which the admittance,  $\mathcal{Y} = I/V$ , of the sample (cell) can be determined. For the case worked out here, it is given by

$$\mathcal{Y} = \frac{Sq}{V_0} [\Phi_+(i\omega)\eta_+(d/2) - \Phi_-(i\omega)\eta_-(d/2)] + i\omega \frac{\epsilon S}{V_0} \frac{d}{dz} \phi(d/2). \quad (23)$$

The impedance connected to Eq. (23) is obtained by using  $Z = 1/\mathcal{Y}$  from which we can obtain  $\epsilon'$  and  $\epsilon''$ . Figure (1) illustrates the quantities  $\epsilon'$  and  $\epsilon''$  obtained from the approach presented above (red line) with  $\bar{\kappa}_+(i\omega, \vartheta) = \bar{\kappa}_-(i\omega, \vartheta) = \bar{\kappa}(i\omega, \vartheta)$ , where  $\bar{\kappa}(i\omega, \vartheta) = \bar{\kappa}(i\omega)\delta(\vartheta-1)$  with  $\bar{\kappa}(i\omega) = \kappa_1\tau/(i\omega\tau)^{\eta_1} + \kappa_2\tau/(i\omega\tau)^{\eta_2}$  and the cases characterized by perfect blocking electrodes (black line)  $\bar{\kappa}(i\omega, \vartheta) = 0$  and adsorption (blue line)  $\bar{\kappa}(i\omega, \vartheta) = \kappa_3\tau_3/(1+i\omega\tau_3)$ . Note that the behavior in the low frequency limit of the model proposed here with different mobilities is very different from the standard cases.

### 3. MODEL AND EXPERIMENTAL DATA

Now, we compare the phenomenological model described above with the experimental data obtained for ionic solutions of  $KClO_3$  (supplied by QEEL - Industrias Químicas S.A. with over 99.9% as received) dissolved in Milli-Q deionized water with the dielectric spectroscopy technique. The measurements of real and imaginary parts of the complex dielectric were performed by using a Solartron SI 1296 A impedance/gain phase analyzer. The frequency range used was from  $10^{-2}$  Hz to 10 kHz. The amplitude of the AC applied voltage was 20 mV. The ionic solutions were placed between two circular surfaces spaced 1.0 mm from each other. The area of electrical electrodes was  $3.14 \text{ cm}^2$ . We used the electrical contact of stainless steel. Before starting the measurements, we adopted the following cleaning procedure: first, the electrodes were washed with detergent and deionized water also polished with fine sandpaper. Then, the electrodes were placed on ultrasonic bath for 10 min. After performing this procedure, the ionic solution, formed by the Milli-Q water with a quantity of the salt  $KClO_3$  completely dissolved, is introduced in the electrodes (1.0 mm thickness) and the real  $\epsilon'$  and the imaginary  $\epsilon''$  part of the complex dielectric constant are measured. This procedure is applied to six ionic solutions of the Milli-Q water with the salt  $KClO_3$  considered here. The six different solutions were prepared with the following salt concentrations: solution (a)  $4.08 \times 10^{-3} \text{ mol L}^{-1}$ ; solution (b)  $1.28 \times 10^{-2} \text{ mol L}^{-1}$ ; (c)  $1.71 \times 10^{-2} \text{ mol L}^{-1}$ ; solution (d)  $4.48 \times 10^{-2} \text{ mol L}^{-1}$ ; solution (e)  $6.85 \times 10^{-2} \text{ mol L}^{-1}$ ; solution (f)  $0.17 \text{ mol L}^{-1}$ .

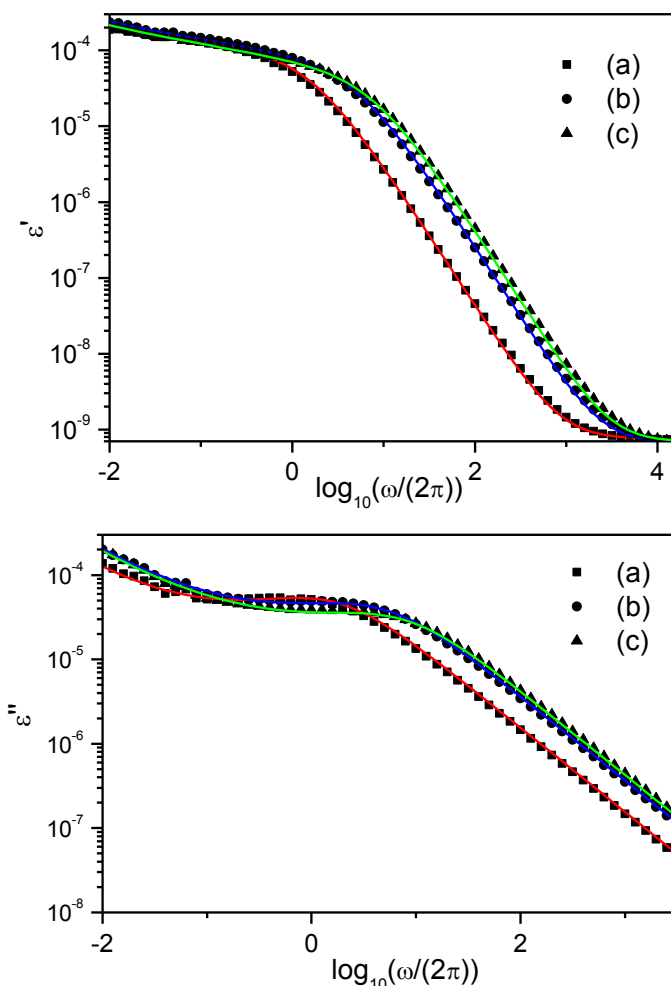


**Figure 2.** Behavior of the real and imaginary parts of the complex dielectric constant for different concentrations is shown. The concentrations used are (a)  $4.08 \times 10^{-3} \text{ mol L}^{-1}$  (black squares), (b)  $1.28 \times 10^{-2} \text{ mol L}^{-1}$  (black circles), and (c)  $1.71 \times 10^{-2} \text{ mol L}^{-1}$  (black triangles), respectively. The experimental data are represented by the black symbols and the model corresponds to the colored solid lines. The values of the parameters for the red solid line are  $\kappa_1 = 2.1 \times 10^{-4} \text{ m/s}$ ,  $\kappa_2 = 7.35 \times 10^{-7} \text{ m/s}$ ,  $\lambda = 3.39 \times 10^{-7} \text{ m}$ ,  $\tau = 5.47 \times 10^{-4} \text{ s}$ ,  $\eta_1 = 0.152$ ,  $\eta_2 = 0.87$ , and  $\epsilon_\infty = 85 \epsilon_\infty$ . For the blue solid line, we have  $\kappa_1 = 6.1 \times 10^{-6} \text{ m/s}$ ,  $\kappa_2 = 3.05 \times 10^{-8} \text{ m/s}$ ,  $\lambda = 2.078 \times 10^{-8} \text{ m}$ ,  $\tau = 0.011 \text{ s}$ ,  $\eta_1 = 0.193$ ,  $\eta_2 = 0.87$ , and  $\epsilon_\infty = 80 \epsilon_\infty$ . The green solid line is obtained by considering  $\kappa_1 = 7 \times 10^{-6} \text{ m/s}$ ,  $\kappa_2 = 2.45 \times 10^{-8} \text{ m/s}$ ,  $\lambda = 1.962 \times 10^{-8} \text{ m}$ ,  $\tau = 5 \times 10^{-3} \text{ s}$ ,  $\eta_1 = 0.22$ ,  $\eta_2 = 0.88$ , and  $\epsilon_\infty = 78 \epsilon_\infty$ .

Figure 2 shows the experimental data, black symbols (square, circle, and triangle), and the model, color solid lines (red, blue, and green), for the real and imaginary parts of the complex dielectric. In order to obtain the agreement between the experimental data and the phenomenological model present in Sec. II, we consider that the dynamic of the processes on the surface are governed by  $\bar{\kappa}_+(i\omega, \mathcal{G}) = \bar{\kappa}_-(i\omega, \mathcal{G}) = \bar{\kappa}(i\omega, \mathcal{G})$ , where  $\bar{\kappa}(i\omega, \mathcal{G}) = \bar{\kappa}(i\omega)\delta(\mathcal{G}-1)$  with  $\bar{\kappa}(i\omega) = \kappa_1\tau/(i\omega\tau)^{\eta_1} + \kappa_2\tau/(i\omega\tau)^{\eta_2}$  being  $\kappa_1\tau$  and  $\kappa_2\tau$  two different characteristic lengths. The bulk (diffusion) equation for the concentrations present in Fig. (2) is considered with,

$\mathcal{D}_+ = 2\mathcal{D}_- = 2 \times 10^{-9} m^2 / s$ ,  $\gamma = 1$ , and  $\mathcal{A} + \mathcal{B} = 1$ . Note that these choices leads to a different behavior from the ones obtained from the usual models based on perfect blocking electrodes or adsorption process characterized by a Langmuir approximation are not suitable to obtain a good agreement with the experimental one. In this sense, it is useful to observe in Fig.(1) the behavior of  $\varepsilon'$  and  $\varepsilon''$  illustrated which evidences that the behavior in the low frequency limit for the standard cases is different from the ones exhibit by the experimental data. These features suggest that the dynamics of the ions in this frequency range has a nonusual diffusion which is essentially governed by the surface effects. In fact, nonusual terms are only considered in the boundary conditions which represents the interaction between the surface and the ions present in bulk. In particular, the phenomenological parameters evidence the presence of two different characteristic lengths  $\kappa_1\tau$  and  $\kappa_2\tau$  which can be connected to the layers of the ions on the electrode surfaces. One of them is closed of the surface and the other is more delocalized and they decrease if the quantity of salt increase (see the Table I).

**Table I:** This table shows the values of the quantities  $\kappa_1\tau$  and  $\kappa_2\tau$ , and  $\lambda$  for the concentrations used in Fig.(2). Note that increase the quantity of salt in the solution decrease the quantities related to adsorption -- desorption process ( $\kappa_1\tau$  and  $\kappa_2\tau$ ) and, also, the Debye length ( $\lambda$ ).

Concentration (mol L <sup>-1</sup> )	4.08□10 <sup>-3</sup>	1.28□10 <sup>-2</sup>	1.71□10 <sup>-2</sup>
$\kappa_1\tau$ (m)	1.14 □10 <sup>-7</sup>	6.71□10 <sup>-8</sup>	3.50□10 <sup>-8</sup>
$\kappa_2\tau$ (m)	4.02□10 <sup>-10</sup>	3.35□10 <sup>-10</sup>	1.22□10 <sup>-10</sup>
$\lambda$ (m)	3.39□10 <sup>-8</sup>	2.07□10 <sup>-8</sup>	1.96□10 <sup>-8</sup>

Let us increase the quantity of salt dissolved in water to 4.48□10<sup>-2</sup> mol L<sup>-1</sup> and to 6.85□10<sup>-2</sup> mol L<sup>-1</sup>, respectively. The behaviors of  $\varepsilon'$  and  $\varepsilon''$  are illustrated in Fig. (3) and similar to the previous case, a good agreement between the experimental data (black symbols) and the phenomenological model (color lines) described above is achieved. For these concentrations, we have considered an additional term in the boundary condition to model the surface effects on the dynamics of the ions; and, for the concentration 6.85□10<sup>-2</sup> mol L<sup>-1</sup>, the value obtained for the parameter  $\gamma$  was greater than one evidencing the presence of finite phase velocity. The additional term to model the surface is given by  $\bar{\kappa}_{add}(i\omega, \mathcal{G}) = \bar{\kappa}_3(i\omega)\delta(\mathcal{G}-1)$  with  $\bar{\kappa}_3(i\omega) = \kappa_3\tau_3/(1+i\omega\tau_3)$ . In order to confirm the presence of  $\gamma > 1$ , we increase the concentration of salt in water to 0.17 mol L<sup>-1</sup>. The results presented in Fig. (4) shown that a suitable behavior is obtained when  $\gamma$  is greater than one, similar to the concentration (e), which suggests a dependence between the concentration of ions and the diffusion process, i.e., the  $\gamma$  values.

#### 4. DISCUSSIONS

We have developed a phenomenological model by considering a fractional diffusion equation of distributed order by taking into account integro-differential boundary conditions. We also

considered different molities, diffusion coefficients, and surface effects. The result obtained from this model was illustrated in Fig. (1) in comparison with the standard cases to illustrate the differences. In particular, the main difference was observed in the low frequency limit where the surface effects, i.e., the boundary conditions, play an important role. In this point, it is also interesting to note that difference between the model analyzed here other developments (see e.g., Ref. [31] and [32]) is that the fractional diffusion equations for the ions are solved taking into account the Poisson equation and integro-differential boundary conditions. In particular, we have the presence of the fractional time derivatives of distributed order in the bulk (diffusion) equation and in the boundary conditions. Thus, we may interpolate several contexts which play an important role describing the electrical response of a system and, consequently, investigate systems where the nonusual behavior is manifested.

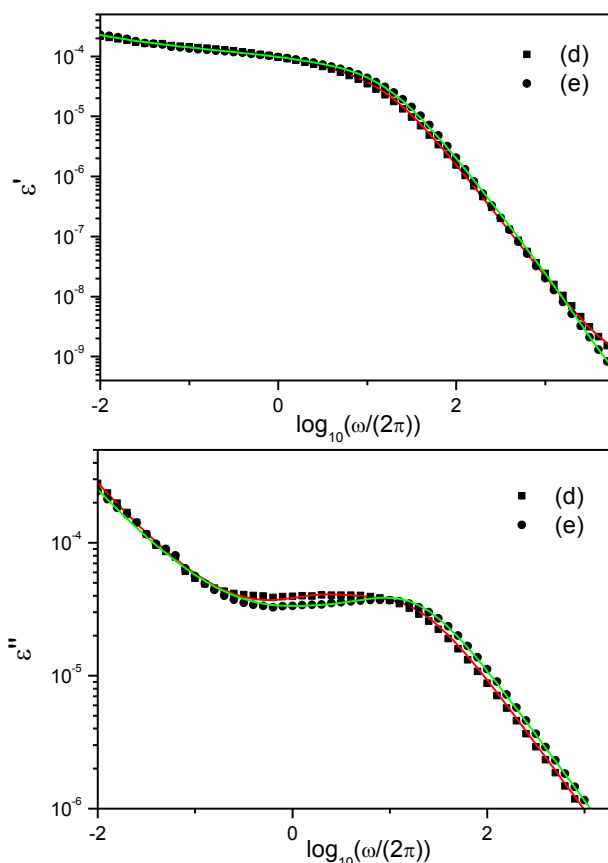


**Figure 3.** Behavior of the real and imaginary parts of the complex dielectric constant for two different concentrations. The concentrations used in (d) and (e) are  $4.48 \times 10^{-2} \text{ mol L}^{-1}$  (black squares) and  $6.85 \times 10^{-2} \text{ mol L}^{-1}$  (black circles), respectively. The experimental data are represented by the black (square and circle) symbols and the model corresponds to the colored (red and green) lines. The values of the parameters for (d) are parameters are  $\kappa_1 = 1.80 \times 10^{-5} \text{ m/s}$ ,  $\kappa_2 = 4.14 \times 10^{-8} \text{ m/s}$ ,  $\kappa_3 = 5.4 \times 10^{-10} \text{ m/s}$ ,  $\lambda = 1.61 \times 10^{-8} \text{ m}$ ,  $\tau = 2.1 \times 10^{-3} \text{ s}$ ,  $\tau_3 = 0.0735 \text{ s}$ ,  $\eta_1 = 0.149$ ,  $\eta_2 = 0.89$ ,  $\gamma = 1$ , and  $M_{\infty} = 78 M_{\infty}$ . For the concentration (e), we have that  $\kappa_1 = 1.65 \times 10^{-5} \text{ m/s}$ ,  $\kappa_2 = 3.79 \times 10^{-8} \text{ m/s}$ ,  $\kappa_3 = 1.188 \times 10^{-10} \text{ m/s}$ ,  $\lambda = 1.59 \times 10^{-8} \text{ m}$ ,  $\tau = 2.1 \times 10^{-3} \text{ s}$ ,  $\tau_3 = 0.0735 \text{ s}$ ,  $\eta_1 = 0.149$ ,  $\eta_2 = 0.865$ ,  $M_{\infty} = 70 M_{\infty}$ ,  $\mathcal{A} = 0.98$ , and  $\gamma = 1.085$ .

By using this model, we have investigated the experimental data of the complex dielectric constant of ionic solutions of  $KClO_3$  dissolved in Milli-Q water. In particular, we compare the phenomenological framework with experimental data as show in Figs. (2), (3), and (4).

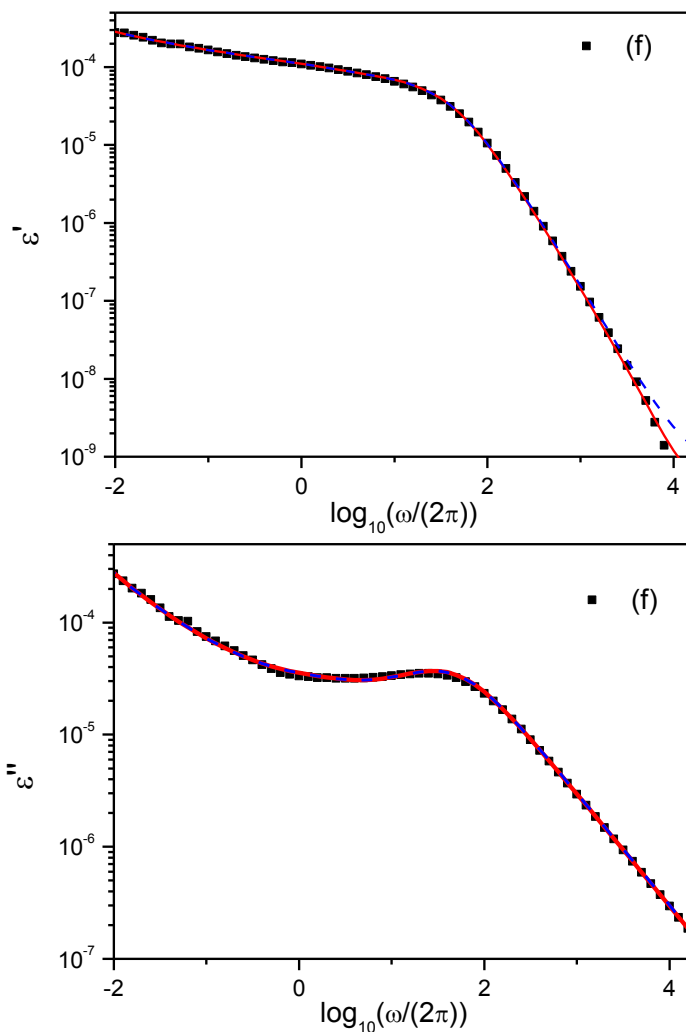


**Figure 4.** Behavior of the real and imaginary parts of the complex dielectric constant versus frequency for the concentration (f)  $0.17 \text{ mol L}^{-1}$ . The experimental data are represented by the black squares and the model with  $\gamma > 1$  corresponds to the solid red line. The values of the parameters for are  $\kappa_1 = 9 \times 10^{-7} \text{ m/s}$ ,  $\kappa_2 = 6.03 \times 10^{-8} \text{ m/s}$ ,  $\kappa_3 = 1.125 \times 10^{-9} \text{ m/s}$ ,  $\lambda = 7.24 \times 10^{-9} \text{ m}$ ,  $\tau = 5 \times 10^{-3} \text{ s}$ ,  $\tau_3 = 0.15 \text{ s}$ ,  $\eta_1 = 0.245$ ,  $\eta_2 = 0.865$ ,  $\mathfrak{M} = 75 \mathfrak{M}_e$ ,  $\mathcal{A} = 0.90$ , and  $\gamma = 1.018$ . The blue dotted line, which corresponds to the model with previous parameter values with  $\gamma = 1$ , was incorporated to evidence in  $\epsilon'$  and  $\epsilon''$  the effect produce by the choice  $\gamma > 1$ .

The agreement between the experimental data present in Fig. (2) and the model is obtained by considering the diffusion equation with  $\gamma = 1$  and the processes on the surface, boundary conditions, governed by a power laws with different thickness,  $\kappa_1\tau$  and  $\kappa_2\tau$ . Following, we increase the

concentration of ions in the solution and the changes were first evidenced on the dynamics of the processes (see Fig. (3)) occurring at the surface. It was necessary to incorporate another term in the boundary condition to obtain a good agreement with the experimental data. This additional term has the thickness,  $\kappa_3\tau_3$ .

Another point is the presence  $\gamma > 1$  in Eq. (1) to fit the experimental data obtained for the concentration (e), in contrast with the results presented in Refs. [27] and [28] characterized by the usual case or  $0 < \gamma < 1$ . The concentration (f) present in Fig. (4) have also required  $\gamma > 1$  to fit the experimental data. These results, supported by the agreement between the experimental data and the model presented in Sec. 2, evidence that the dynamics of the ions in the sample is not usual and may be related to the diffusive regimes which can be suitably described if the boundary conditions and the bulk equation are modified.

## 5. CONCLUSIONS

The results obtained in the framework developed here, in Sec. 2, exhibit a rich class of behaviors depending on the choices performed for boundary conditions, i.e., for the function  $\bar{\kappa}_\alpha(t, \vartheta)$ , as shown in Fig. 1. The index  $\gamma$  of the fractional time derivative present in the diffusion equation can also modify the behavior electrical response. This manner the approach analyzed here may describe scenarios characterized by different diffusive behaviors such as, for example, the discussed in Refs. [27-29]. In this sense, the comparison between the experimental data and the model performed in Sec. 3 suggests that dynamic of the ions present different diffusive regimes. Finally, we also hope that the results presented here can be useful to investigate the electrical response of others systems and their connections with the anomalous diffusion.

## ACKNOWLEDGEMENT

This work was partially supported by the National Institutes of Science and Technology (INCT-CNPq) of Complex Systems and Complex Fluids. We also thank Fundação Araucária.

## References

1. R. Brown, in *The Miscellaneous Botanical Works of Robert Brown*, edited by John J. Bennett, Vol. 1, London, 1866.
2. A. Einstein, *Ann. Phys. (Leipzig)*, 17 (1905) 549.
3. P. Brault, C. Jossierand, J. M. Bauchire, A. Caillard, C. Charles, and R. W. Boswell, *Phys. Rev. Lett.*, 102 (2009) 045901.
4. Yoav Sagi, Miri Brook, Ido Almog, and Nir Davidson, *Phys. Rev. Lett.*, 108 (2012) 093002.
5. Y. Caspi, D. Zbaida, H. Cohen, and M. Elbaum, *Macromolecules*, 42 (2009) 760.
6. C. D. Ball, N. D. MacWilliam, J. K. Percus, and R. K. Bowles, *J. Chem. Phys.*, 130 (2009) 054504.
7. M Burgis, V Schaller, M Glässl, B Kaiser, W Köhler, A Krekhov, and W Zimmermann, *New Journal of Physics*, 13 (2011) 043031.

8. V. V. Saenko, *Plasma Phys. Rep.*, 35 (2009) 1.
9. R.A. Pfafenzeller, E. Lenzi, M.K. Lenzi, *Int. Rev. Chem. Eng.*, 3 (2011) 818.
10. B. O'Shaughnessy and I. Procaccia, *Phys. Rev. Lett.*, 54 (1985) 455.
11. R. Metzler, G. Glockle and T. F. Nonnenmacher, *Physica A*, 211 (1994) 13.
12. A. Mertelj, L. Cmok, and M. Copic, *Phys. Rev. E*, 79 (2009) 041402.
13. H. Randariamahazaka, V. Noel, and C. Chevrot, *J. Elect. Chem.*, 556 (2003) 35.
14. R. Golestanian, *Phys. Rev. Lett.*, 102 (2009) 188305.
15. Maayan Lia Yizraeli and Daphne Weihs, *Cell. Biochem. Biophys.*, 61 (2011) 605.
16. C. W. Gardiner, *Handbook of Stochastic Methods: For Physics, Chemistry and the Natural Sciences, Springer Series in Synergetics*, Springer, New York, 1996.
17. A. Pekalski and K. Sznajd-Weron Eds., *Anomalous Diffusion: From Basics to Applications*, Lecture Notes in Physics, Springer, Berlin, 1999.
18. R. Metzler and J. Klafter, *Phys. Rep.*, 339 (2000) 1.
19. R. Hilfer, *Applications of Fractional Calculus in Physics*, World Scientific, Singapore, 2000.
20. F. Bouchet and J. Barré, *Journal Physics: Conference Series*, 31 (2006) 18.
21. V. Latora, A. Rapisarda, and S. Ruffo, *Phys. Rev. Lett.*, 83 (1999) 2104.
22. V. Latora, A. Rapisarda, and C. Tsallis, *Phys. Rev. E*, 64 (2001) 056134.
23. E. K. Lenzi, L. R. Evangelista, and G. Barbero, *Europhysics Lett.*, 85 (2009) 28004.
24. E. K. Lenzi, C. A. R. Yednak, and L. R. Evangelista, *Phys. Rev. E*, 81 (2010) 011116.
25. S. Sunde, I. A. Lervik, M. Tsyppkin, and Lars-Erik Owe, *Electrochimica Acta*, 55 (2010) 7751.
26. F. Batalioto, A. R. Duarte, G. Barbero, and A. M. F. Neto, *J. Phys. Chem. B*, 114 (2010) 3467.
27. E. K. Lenzi, P. R. G. Fernandes, T. Petrucci, H. Mukai, and H. V. Ribeiro, *Phys. Rev. E*, 84 (2011) 041128.
28. F. Ciuchi, A. Mazzulla, N. Scaramuzza, E. K. Lenzi, and L. R. Evangelista, *J. Phys. Chem. C*, 116 (2012) 8773.
29. D. L. Sidebottom, *Rev. Mod. Phys.*, 81 (2009) 999.
30. T. Basu, M. M. Goswami, T. R. Middya, and S. Tarafdar, *J. Phys. Chem. B*, 116 (2012) 11369.
31. J. Bisquert and A. Compte, *J. Electroanalytical Chemistry*, 499 (2001) 112.
32. J. Bisquert, G. Garcia-Belmonte, and A. Pitarch, *Chem. Phys. Chem.*, 4 (2003) 287.
33. J. Bisquert, *Phys. Rev. E*, 72 (2005) 011109.
34. J. Bisquert, *Phys. Rev. Lett.*, 91 (2003) 010602.
35. E. K. Lenzi, L. R. Evangelista, and G. Barbero, *J. Phys. Chem. B*, 113 (2009) 11371.
36. J. R. Macdonald, L. R. Evangelista, E. K. Lenzi, and G. Barbero, *J. Phys. Chem. C*, 115 (2011) 7648.
37. P. A. Santoro, J. L. de Paula, E. K. Lenzi, and L. R. Evangelista, *J. Chem. Phys.*, 135 (2011) 114704.
38. J.T. Machado, V. Kiryakova, and F. Mainardi, *Commun. Nonlinear Sci.*, 16 (2011) 1140.
39. R. Hilfer, R. Metzler, A. Blumen, and J. Klafter (Eds.), Strange Kinetics, *Chemical Physics* 284 (2002) pp. 1 - 541.
40. J. Klafter, S. C. Lim, and R. Metzler (Eds.), *Fractional Dynamics: Recent Advances*, World Scientific Publishing Company, Singapore, 2011.
41. E. K. Lenzi, R. S. Mendes, and C. Tsallis, *Phys. Rev. E*, 67 (2003) 031104.
42. I. M. Sokolov, *Phys. Rev. E*, 66 (2002) 041101.
43. P. C. Assis, Jr., R. P. de Souza, P. C. da Silva, L. R. da Silva, L. S. Lucena, and E. K. Lenzi, *Phys. Rev. E*, 73 (2006) 032101.
44. T. Srokowski, *Phys. Rev. E*, 75 (2007) 051105.
45. I. Podlubny, *Fractional Differential Equations*, (Academic Press, San Diego, 1999).
46. G. Barbero and L. R. Evangelista, *Adsorption Phenomena and Anchoring Energy in Nematic Liquid Crystals*, Taylor & Francis, London, 2006.
47. R. K. Saxena, A. M. Mathai, and H. J. Haubold, *J. Math. Phys.*, 51 (2010) 103506.

48. V. G. Gupta, B. Sharma, and F. B. M. Belgacem, *App. Math. Science*, 5 (2011) 899 .
49. T. C. Halsey and M. Leibic, *Annals of Physics*, 219 (1992) 109.
50. L. Nyikos and T. Pajkossy, *Electrochimica Acta*, 30 (1985) 1533.